

Review

# Ion Trap Quantum Computers Part 1: 1-Qubit Gates

Bernd Baumann 

Heinrich Blasius Institute of Physical Technologies, Hamburg University of Applied Sciences, Berliner Tor 21, 20099 Hamburg, Germany  
Email: info@berndbaumann.de

Received: 28 March 2025; Accepted: 21 April 2025; Published: 27 May 2025

**Abstract:** Ions offer a promising approach to physically realize qubits. The present text extensively elucidates the physics of 1-qubit gates for use in quantum computers based on ion qubits. To keep the discussion as simple as possible, ions are treated mechanically as rigid rotors. The discussed system is excellently suited to practice important elementary methods of quantum physics using a practical application example. For didactic reasons, contrary to the usual approach, a typographical distinction is made between states and operators on the one hand and column vectors and matrices on the other. The article is aimed at readers with basic knowledge of quantum physics, i.e., those familiar with terms like Schrödinger equation, wave function, bra and ket, Pauli matrices, and the like. Rudimentary knowledge of quantum computers is also assumed (qubit, gate, ...).

**Keywords:** quantum physics; quantum computer; ion trap; quantum gate

---

## 1. Introduction

For several decades, quantum physics has been undergoing a phase commonly referred to as the second quantum revolution [1,2]. Advances in measurement techniques allow quantum phenomena, initially only indirectly detectable, to now be observed directly. Moreover, ideas are being formulated and implemented to make bizarre phenomena like superposition and entanglement usable for technical purposes. One of these technical applications is the quantum computer [3–6]. Despite intensive efforts in laboratories of many companies and universities, quantum computers are still in an early stage of development. A recent report estimates that quantum computing alone will lead to about \$1 trillion in value creation within the next 10 years and the formation of 840,000 new jobs in the same period of time [7]. The second quantum revolution is far from over but is in full swing.

The quantum computers existing today are still very rudimentary. Research groups worldwide are searching for the best solutions to various problems that currently hinder progress towards practical quantum computers. One of the remaining questions is which physical system is best suited for realizing qubits.

During the last years IBM as well as Alphabet have made impressive progress by using superconducting transmon qubits. IBM's most recent quantum processor comprises more than 1,000 qubits. Google's quantum processor contains only 105 qubits, but features superior error correction capabilities. The probably most prominent example of a prototypical quantum computer application is prime factorization using Shor's algorithm [8]. The fact that the factorization of a 2048-bit number requires several million qubits illustrates the gap between the present state of the technology and devices for real-world applications. Still, the industry is optimistic to close this gap within a few years.

There are several other well established possibilities for the physical realization of qubits (photons, quantum dots, spin of atoms, ...) and new approaches like transition metal complexes [6,9]. For example vanadyl derivatives feature long coherence times, hyperfine coupling in a suitable

wavelengths range and other favorable properties [10]. It will take a few years to decide whether this class of qubits offer an advantage over established approaches when applied to real world problems.

A further promising qubit candidate is an ion trapped in an ion trap [11]. Companies pursuing this approach are IonQ and Quantinuum (Merger of Cambridge Quantum and Honeywell Quantum Solutions). This article extensively presents the quantum physics of the ion trap quantum computer using a highly simplified ion model [12–14]. The quantum effect employed in the first part, focusing on 1-qubit gates, is the superposition  $|\psi\rangle = a|0\rangle + b|1\rangle$  of the two logical basis states  $|0\rangle$  and  $|1\rangle$ . In the second part (2-qubit gates using the CNOT gate as an example), the entanglement effect is added. The presentation here is inspired by B. Zygelman [5].

The scenario described in this first part of the article is as follows: An ion is trapped in an ion trap and is initially brought into its energetic ground state by cooling. The logical qubit state  $|0\rangle$  is assigned to the ground state. A quantum gate has the task of transforming this state into a specific well-defined superposition state with an energetically excited state. In the ion trap quantum computer, this is achieved by exposing the ion to laser radiation. To generate the specified superposition state, the radiation must have very precisely defined properties in terms of propagation direction, wavelength (or frequency), and polarization. The duration of the irradiation is also essential. The following sections will focus on calculating how to choose the parameters of the laser radiation to generate a given superposition state of the ion.

The calculations are sometimes a bit tedious. Readers who want to follow them in detail may find the use of a computer algebra system (Mathematica®, Maple®, Maxima, ...) helpful.

## 2. The Rotor Model

So the qubits shall be realized using ions. In order to keep the quantum physical treatment of the system as simple as possible, an ion consisting of a positively charged nucleus and a single, negatively charged electron is to be used as the qubit. In the context of the classical, non-quantum physical description, it is also assumed that the electron orbits the nucleus of the ion at a fixed distance  $R$  ('model of the *rigid rotor*').

In the case considered here, it is a mechanical system consisting of two point masses that are firmly connected by a rigid and massless axis (Figure 1). Since the mass of the nucleus  $M$  is several thousand times the mass of the electron  $m$ , the center of gravity of the system almost coincides with the center of gravity of the nucleus. The center of gravity of the system is assumed to be at rest. The motion of the electron is restricted to the  $x - y$  plane of the coordinate system used. Under these conditions, the only possible movement is a rotational movement of the electron around the coordinate origin. The angular velocity  $\omega$  is linked to the modulus of the velocity  $v := |\vec{v}|$  by  $v = R\omega$ . A negative/positive value of  $\omega$  indicates, whether the electron rotates clockwise/counterclockwise.

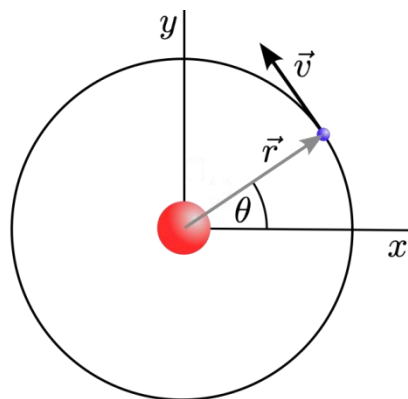


**Figure 1.** Schematic representation of a rotor. The electron moves at a fixed distance  $R := |\vec{r}| = \text{const}$  around the coordinate origin.

According to the laws of classical physics, any value is allowed for the angular velocity ( $-\infty \leq \omega \leq \infty$ ) (We consider the non-relativistic case). The energy of the rotor can be expressed in the form

$$E = E_{\text{rot}} = \frac{1}{2}J\omega^2.$$

Here  $J$  denotes the moment of inertia, which in this case is given by  $J = mR^2$ . Obviously, the energy can assume any non-negative value ( $0 \leq E_{\text{rot}} \leq \infty$ ). Since the motion of the electron is restricted to the  $x - y$  plane, the angular momentum  $\vec{L}$  points in the  $z$  direction. The corresponding component of the angular momentum is

$$L_z = J\omega.$$

For the transition to quantum physics, the Hamiltonian function, i.e. the energy, expressed as a function of the canonical variables, is required (see [15] Lectures 6 and 8). In the present case, the energy depends on the canonical momentum  $L_z$ , but not on the canonical coordinate (which would be the angle  $\theta$ ):

$$E_{\text{rot}} = \frac{1}{2}(J\omega)\omega = \frac{L_z^2}{2J}$$

and consequently

$$H(L_z) = \frac{L_z^2}{2mR^2}.$$

The corresponding Hamiltonian operator therefore has the form (We will use bold characters throughout for quantum physical operators)

$$\mathbf{H}(\mathbf{L}_z) = \frac{1}{2mR^2} \mathbf{L}_z^2. \tag{1}$$

An operator  $\mathbf{A}$  maps a quantum mechanical state  $|\psi\rangle$  according to

$$|\phi\rangle = \mathbf{A}|\psi\rangle \tag{2}$$

to a state  $|\phi\rangle$ . The corresponding position representation of this equation is obtained by forming the scalar product

$$\langle x|\phi\rangle = \langle x|\mathbf{A}|\psi\rangle$$

( $|x\rangle$  is an eigenstate of the position operator  $\mathbf{x}$ ). If  $\mathbf{A}$  is the momentum operator  $\mathbf{p}_x$  corresponding to the position operator  $\mathbf{x}$ , it can be shown that the wave function  $\phi(x) = \langle x|\phi\rangle$  of the state  $|\phi\rangle$  can be calculated from the  $x$ -derivative of the wave function  $\psi(x) = \langle x|\psi\rangle$  of the state  $|\psi\rangle$  (cf. [16] Section 1.7):

$$\langle x|\mathbf{p}_x|\psi\rangle = -i\hbar \frac{\partial}{\partial x} \langle x|\psi\rangle$$

( $\hbar$  reduced Planck constant,  $i$  imaginary unit).

For rotational motion, and hence also for the case of the rotor discussed above, an analogous relationship applies. It reads (cf. [16] Section 3.6)

$$\langle \theta|\mathbf{L}_z|\psi\rangle = -i\hbar \frac{\partial}{\partial \theta} \langle \theta|\psi\rangle$$

( $|\theta\rangle$  is an eigenstate of the angular operator  $\boldsymbol{\theta}$  (see Figure 1)). In position representation, the Hamiltonian operator of the rotor can thus be written in the form

$$\langle \theta|\mathbf{H}|\psi\rangle = -\frac{\hbar^2}{2mR^2} \frac{\partial^2}{\partial \theta^2} \langle \theta|\psi\rangle$$

(cf. [16] Section 1.7).

Now, the quantum physically allowed results of measurements of angular momentum and energy are to be determined. Therefore, the eigenvalues of the corresponding operator have to be calculated. For the  $z$ -component of angular momentum, the eigenvalue equation in position representation reads

$$-i\hbar \frac{\partial}{\partial \theta} \psi(\theta) = L_z \psi(\theta)$$

$(\psi(\theta) = \langle \theta | \psi \rangle)$ . The solution to this differential equation is well known to be

$$\psi(\theta) = c_1 \exp(iL_z \theta / \hbar),$$

where  $c_1$  represents the integration constant.

The angular position  $\theta$  and all angles differing from  $\theta$  by an integer multiple of  $2\pi$  denote the same location in space. Hence, it must hold that (A better justification for the integrality of  $\ell$  can be found in [16] Section 3.5)

$$\psi(\theta) = \psi(\theta + 2\pi\ell) \quad \text{with } \ell \in \{\pm 1, \pm 2, \dots\}.$$

From this condition, it follows that the allowed values of the  $z$ -component of angular momentum are given by

$$L_z = \ell \hbar.$$

The sign of  $\ell$  is associated with the sense of rotation of the electron according to the convention introduced above. Thus, the eigenfunctions of the  $z$ -component of angular momentum have the simple form:

$$\psi_\ell(\theta) = c_1 \exp(i\ell\theta) \quad \text{with } \ell \in \{\pm 1, \pm 2, \dots\}. \tag{3}$$

To calculate the allowed energy values of the rotor, one needs to solve the time-independent Schrödinger equation

$$\mathbf{H}|\psi\rangle = E|\psi\rangle.$$

For the present problem, this equation in position representation takes the form

$$-\frac{\hbar^2}{2mR^2} \frac{\partial^2}{\partial \theta^2} \psi(\theta) = E\psi(\theta). \tag{4}$$

Since the Hamiltonian operator from Equation (1) commutes with  $L_z$ , the eigenfunctions from Equation (3) are also eigenfunctions of Equation (4). It is important to note that states differing only by the sense of rotation have the same energy. The energy eigenfunctions are superpositions of these two angular momentum states:

$$\psi_{E_\ell}(\theta) = c_2 \exp(+i\ell\theta) + c_3 \exp(-i\ell\theta). \tag{5}$$

$c_2$  and  $c_3$  are integration constants again. Substituting the solution into the differential equation yields the allowed energy values:

$$E_\ell = \frac{(\hbar\ell)^2}{2mR^2}.$$

For the energy difference  $\Delta E_\ell := E_{\ell+1} - E_\ell$  between neighboring energy eigenvalues, one obtains

$$\Delta E_\ell = \frac{\hbar^2}{2mR^2} (2\ell + 1). \tag{6}$$

Thus, the spacing between neighboring energy eigenvalues increases linearly with the quantum number  $\ell$ .

The solution (5) of the differential equation (4) can be expressed in the usual manner in real form ([17] Section 2.4):

$$\psi_{E_\ell}(\theta) = c_4 \sin(\ell\theta) + c_5 \cos(\ell\theta).$$

In the following, the special case  $c_5 = 0$  and  $\ell \in \{+1, +2, \dots\}$  (counterclockwise rotation) will be considered. From the normalization condition ( $\psi_{E_\ell}^*$  is the complex conjugate of  $\psi_{E_\ell}$ )

$$\int_0^{2\pi} \psi_{E_\ell}^* \psi_{E_\ell} d\theta = 1$$

the integration constant  $c_4$  is determined. Therefore:

$$\psi_{E_\ell}(\theta) = \frac{1}{\sqrt{\pi}} \sin(\ell\theta). \tag{7}$$

The functions  $\psi_{E_\ell}(\theta)$  represent the position representations of the energy eigenstates  $|E_\ell\rangle$ . These states are orthonormal:

$$\langle E_\ell | E_{\ell'} \rangle = \delta_{\ell\ell'}$$

( $\delta_{\ell\ell'}$  Kronecker delta). The probability densities  $\psi_{E_\ell}^* \psi_{E_\ell}$  of the electron as a function of the angle  $\theta$  are shown for  $\ell = 1$  and  $\ell = 2$  in Figure 2.

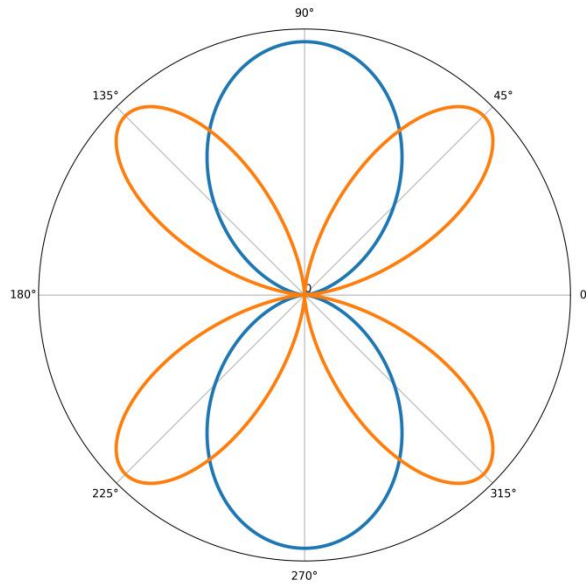


**Figure 2.** Probability density of the electron for  $\ell = 1$  (blue) and  $\ell = 2$  (orange). The probability corresponds to the length of the line from the origin to the respective curve at the corresponding angle.

For time-independent Hamiltonian operators, any time-dependent state can be formed from the stationary solutions (7) of the time-independent Schrödinger equation (4) by superposition:

$$|\psi(t)\rangle = \sum_{\ell=1}^{\infty} C_\ell |E_\ell\rangle \exp(-iE_\ell t/\hbar). \tag{8}$$

The coefficients  $C_\ell$  are determined by the initial conditions ([16] Section 2.1).

### 3. Excitation by Laser Radiation

For the following, it is assumed that an electromagnetic wave propagates along the  $z$ -axis of the coordinate system. The radiation field is generated by a laser and falls perpendicularly to the plane of rotation of the electron onto the rotor ion. Its electric component in the  $x - y$  plane, where the ion is located, is described by

$$\vec{E}(t) = \hat{E} (\cos(\omega t + \delta) \vec{e}_x + \sin(\omega t) \vec{e}_y). \tag{9}$$

It thus depends on time, but not on position (i.e., on  $x$  or  $y$ ). Among other things, this means that the diameter of the laser beam is assumed to be much larger than the diameter of the electron's orbit. The magnetic field component is neglected.

In Figure 3, the temporal behavior of the electric field for various values of  $\delta$  is illustrated. The path of the tip of the vector  $\vec{E}(t)$  which is attached to any point in the  $x - y$  plane, is shown. For example, in the case of  $\delta = 0$ , it is easy to see that it is possible to align the directions of  $\vec{E}(t)$  with the direction of the velocity vector of the electron  $\vec{v}(t)$  throughout the entire orbit. This requires that  $\omega$  and the angular velocity of the electron, as well as the temporal phase relationship between the

two vectors, match. In this case, the electron will experience a constant acceleration under the influence of the field, and its energy will steadily increase (More precisely, due to the negative charge of the electron, the directions of the two vectors must be opposite). The angular frequency must constantly be adjusted to match the electron’s angular frequency. For  $\delta = \pi/2$ , acceleration still occurs in a periodic rhythm under the appropriate conditions. The acceleration is maximum for the angular positions  $\pi/4$  and  $3\pi/4$ .

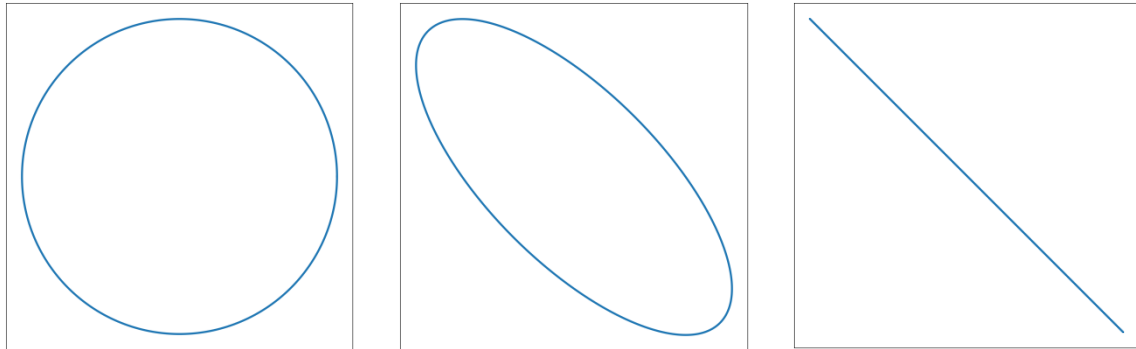


**Figure 3.** The path of the tip of the field strength vector over one period  $T = 2\pi/\omega$  for  $\delta = 0$ ,  $\delta = \pi/4$ ,  $\delta = \pi/2$  (from left to right).

The considerations of the previous section were purely classical in nature. The following will focus on what statements quantum physics makes regarding the excitation of rotor ions by laser radiation.

We assume that the rotor ion is in the ground state  $|E_1\rangle$ . This can be achieved, for example, by cooling. Its energy is

$$E_1 = \frac{\hbar^2}{2mR^2}.$$

Excitation of the ion is only possible if the frequency of the radiation satisfies the resonance condition  $\omega = (E_{\ell'} - E_{\ell})/\hbar$ . For energetically neighboring levels, this can be expressed in the form

$$\omega = \omega_{\ell} := \frac{\Delta E_{\ell}}{\hbar}. \tag{10}$$

To induce a transition from the ground state to the first excited state  $|E_2\rangle$ , the frequency of the laser radiation must therefore be set to

$$\omega_1 = \frac{3\hbar}{2mR^2}. \tag{11}$$

Since the energy differences depend on  $\ell$  due to Equation (6), the radiation will not raise the excited ion to the next higher energy state  $|E_3\rangle$ . Instead, the ion will return to the ground state through stimulated emission and spontaneous emission (see [18] Chapter 4). This is followed by reabsorption of radiation; the system constantly oscillates between the states  $|E_1\rangle$  and  $|E_2\rangle$  (Rabi oscillations).

As long as the frequency of the laser radiation is kept at the value  $\omega_1$ , only the two lowest energy states are involved in all processes. In this case a general time-dependent state is described instead of Equation (8) by

$$|\psi(t)\rangle = C_1|E_1\rangle \exp(-iE_1t/\hbar) + C_2|E_2\rangle \exp(-iE_2t/\hbar). \tag{12}$$

This finally allows the connection to the topic of quantum computers: The two energy states  $|E_1\rangle$  and  $|E_2\rangle$  are used as logical qubit states  $|0\rangle$  and  $|1\rangle$ . Therefore, in the following, we write  $|b\rangle$  or  $|b'\rangle$  with  $b, b' \in \{0,1\}$  instead of the kets  $|E_{\ell}\rangle$  with  $\ell \in \{1,2\}$ .

#### 4. Matrix Representation

In quantum physics, two-state systems are most conveniently described in matrix representation. This arises from the following considerations: A general state of a two-state system has the form

$$|\psi\rangle = \psi_0|0\rangle + \psi_1|1\rangle. \tag{13}$$

If the complex expansion coefficients  $\psi_0$  and  $\psi_1$  are combined in a column vector

$$\underline{\psi} = \begin{pmatrix} \psi_0 \\ \psi_1 \end{pmatrix}$$

then the column vectors

$$\begin{pmatrix} 1 \\ 0 \end{pmatrix} \quad \text{and} \quad \begin{pmatrix} 0 \\ 1 \end{pmatrix}$$

clearly represent the qubit states  $|0\rangle$  and  $|1\rangle$ .

A linear mapping of the type represented by Formula (2) corresponds to a linear system of equations

$$\underline{\phi} = \underline{A}\underline{\psi} \quad \text{or} \quad \phi_{b'} = \sum_{b=0}^1 A_{b'b} \psi_b \tag{14}$$

with a  $2 \times 2$  matrix

$$\underline{A} = \begin{pmatrix} A_{00} & A_{01} \\ A_{10} & A_{11} \end{pmatrix}.$$

The state  $|\phi\rangle$  is associated with the column vector

$$\underline{\phi} = \begin{pmatrix} \phi_0 \\ \phi_1 \end{pmatrix}.$$

The system of equations (14) represents formula (2) in the basis defined by  $|0\rangle$  and  $|1\rangle$ .

Using the completeness relation for the reduced state space

$$\mathbf{1} = \sum_{b=0}^1 |b\rangle\langle b|,$$

we have

$$|\psi\rangle = \sum_{b=0}^1 |b\rangle\langle b|\psi\rangle.$$

Comparing with formula (13), we obtain the expansion coefficients of the state vector  $|\psi\rangle$  in the chosen basis:

$$\psi_0 = \langle 0|\psi\rangle \quad \text{and} \quad \psi_1 = \langle 1|\psi\rangle$$

(similarly for  $|\phi\rangle$ ). The matrix elements  $A_{b'b}$  of the operator  $\mathbf{A}$  are determined accordingly:

$$\langle b'|\phi\rangle = \langle b'|\mathbf{A}|\psi\rangle = \sum_{b=0}^1 \langle b'|\mathbf{A}|b\rangle\langle b|\psi\rangle.$$

Comparing with Formula (14), we get

$$A_{b'b} = \langle b'|\mathbf{A}|b\rangle.$$

Important examples of matrices in quantum physics in general and in what follows are the three Pauli matrices

$$\underline{\sigma}_x = \begin{pmatrix} 0 & 1 \\ 1 & 0 \end{pmatrix}, \quad \underline{\sigma}_y = \begin{pmatrix} 0 & -i \\ i & 0 \end{pmatrix} \quad \text{and} \quad \underline{\sigma}_z = \begin{pmatrix} 1 & 0 \\ 0 & -1 \end{pmatrix}$$

alongside the identity matrix

$$\underline{1} = \begin{pmatrix} 1 & 0 \\ 0 & 1 \end{pmatrix}.$$

### 5. Bloch Sphere and Rotation Matrices

We expressed a general state above in the form  $|\psi\rangle = \psi_0|0\rangle + \psi_1|1\rangle$ . The complex coefficients  $\psi_0 = u_0 + iv_0$  and  $\psi_1 = u_1 + iv_1$  correspond to four degrees of freedom. The real numbers  $u_0, u_1, v_0$  and  $v_1$  span a 4-dimensional space.

From the two coefficients  $\psi_0$  and  $\psi_1$ , we obtain the probabilities  $P_b = |\psi_b|^2$  for the occurrence of the associated basis states  $|b\rangle$  when a measurement is performed on the qubit. This assumes that the state  $|\psi\rangle$  is normalized:  $|\psi_0|^2 + |\psi_1|^2 = u_0^2 + v_0^2 + u_1^2 + v_1^2 = 1$ . Thus, out of the four degrees of freedom, only three are independent. All states that differ only by a phase factor  $e^{i\varphi}$  are physically equivalent, since the associated probabilities  $P_b$  are identical. Therefore, the number of degrees of freedom can be further reduced by fixing  $\varphi$  to any value.

Without going into detail, we note that a general state can be written in the form

$$|\psi\rangle = \cos(\beta/2)|0\rangle + e^{i\alpha}\sin(\beta/2)|1\rangle$$

( $0 \leq \alpha < 2\pi, 0 \leq \beta < \pi$ ) (Further details can be found in [5] Section 2.1.2). The two real quantities  $\alpha$  and  $\beta$  can be interpreted as spherical coordinates in a 3-dimensional, abstract state space. The state  $|\psi\rangle$  is uniquely associated with the point  $\vec{b} = (\cos\alpha \sin\beta, \sin\alpha \sin\beta, \cos\beta)^T$  on the surface of the unit sphere in this space, as shown in Figure 4 (The superscript  $T$  denotes the transposed vector). This sphere is known as the Bloch sphere; the unit vector  $\vec{b}$  is called the Bloch vector.

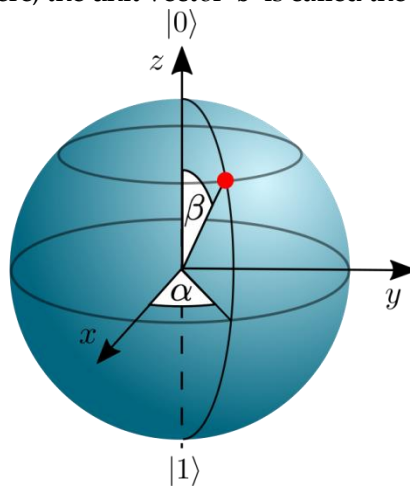


**Figure 4.** The Bloch sphere. The North Pole corresponds to the state  $|0\rangle$ , the South Pole to the state  $|1\rangle$ . Any point on the surface of the sphere corresponds to a superposition state  $|\psi\rangle = \cos(\beta/2)|0\rangle + e^{i\alpha}\sin(\beta/2)|1\rangle$ . Note: The sphere is embedded in the state space, not the physical space!

A matrix that plays an interesting and important role in this context is (cf. [6] Section 4.2)

$$R_z(\gamma) = \exp\left(-\frac{i\gamma\sigma_z}{2}\right).$$

The exponential function of a matrix is defined through its power series expansion, in this case:

$$\exp(-i\gamma\sigma_z/2) = \underline{1} - i(\gamma/2)\sigma_z - \frac{(\gamma/2)^2}{2!}\sigma_z^2 + i\frac{(\gamma/2)^3}{3!}\sigma_z^3 + \dots$$

It is easy to verify that  $\sigma_z^2 = \underline{1}$ . Therefore, we have

$$R_z(\gamma) = \underline{1} \left(1 - \frac{(\gamma/2)^2}{2!} + \dots\right) - i\sigma_z \left(\gamma/2 - \frac{(\gamma/2)^3}{3!} + \dots\right) = \underline{1} \cos(\gamma/2) - i\sigma_z \sin(\gamma/2)$$

and consequently

$$R_z(\gamma) = \begin{pmatrix} \cos(\gamma/2) - i\sin(\gamma/2) & 0 \\ 0 & \cos(\gamma/2) + i\sin(\gamma/2) \end{pmatrix} = \begin{pmatrix} \exp(-i\gamma/2) & 0 \\ 0 & \exp(+i\gamma/2) \end{pmatrix}. \quad (15)$$

Suppose the state  $|\psi\rangle$  is represented by a point on the surface of the Bloch sphere, with azimuthal angle  $\alpha$  and polar angle  $\beta$ . Let the corresponding column vector be  $\underline{\psi}$ . Applying the matrix  $\underline{R}_z(\gamma)$  to  $\underline{\psi}$  moves the associated point on the circle of latitude to azimuthal angle  $\alpha + \gamma$ . The polar angle  $\beta$  remains unchanged. Thus,  $\underline{R}_z(\gamma)$  induces a rotation about the z-axis of the statespace. We therefore refer to  $\gamma$  as the rotation angle. It is evident and easy to confirm using Equation (15) that  $\underline{R}_z(-\gamma)$  is the inverse matrix of  $\underline{R}_z(\gamma)$ :

$$\underline{R}_z^{-1}(\gamma) = \underline{R}_z(-\gamma). \tag{16}$$

Typically, calculations on a quantum computer start with qubits in the ground state (at the North Pole of the Bloch sphere). Applying the rotation matrix  $\underline{R}_z(\gamma)$  to the column vector representing this state, leaves the vector unaltered. However, besides the matrix  $\underline{R}_z$  discussed so far, there are also matrices that induce rotation about the  $x$  or  $y$ -axis:

$$\underline{R}_x(\gamma) = \exp(-i\gamma\underline{\sigma}_x/2) = \begin{pmatrix} \cos(\gamma/2) & -i\sin(\gamma/2) \\ -i\sin(\gamma/2) & \cos(\gamma/2) \end{pmatrix}$$

and

$$\underline{R}_y(\gamma) = \exp(-i\gamma\underline{\sigma}_y/2) = \begin{pmatrix} \cos(\gamma/2) & -\sin(\gamma/2) \\ \sin(\gamma/2) & \cos(\gamma/2) \end{pmatrix}.$$

Starting from the North Pole of the Bloch sphere, any point on the surface of the sphere can be reached by successively applying two of the three rotation matrices  $\underline{R}_x$ ,  $\underline{R}_y$ , and  $\underline{R}_z$ . The rotation matrices will play an important role in the next section.

## 6. Qubit Dynamics

### 6.1. The Free Rotor

Applying the procedure described in Section 4 to the time-dependent Schrödinger equation

$$i\hbar \frac{\partial}{\partial t} |\psi(t)\rangle = \mathbf{H}|\psi(t)\rangle,$$

yields the linear differential equation system

$$i\hbar \dot{\underline{\psi}}(t) = \underline{H}\underline{\psi}(t). \tag{17}$$

Equations (17) and (14) are formally identical, with the correspondence  $\underline{\phi} \leftrightarrow i\hbar \dot{\underline{\psi}}(t)$ ,  $\underline{A} \leftrightarrow \underline{H}$ , and  $\underline{\psi} \leftrightarrow \underline{\psi}(t)$ . The dot above the symbol as usually denotes the time derivative:

$$\dot{\underline{\psi}}(t) = \frac{\partial}{\partial t} \begin{pmatrix} \psi_0(t) \\ \psi_1(t) \end{pmatrix}.$$

The solution of the system of differential equations determines the time evolution of the probabilities to obtain the bit state  $b$  upon measurement of the system:

$$P_b(t) = |\langle b|\psi(t)\rangle|^2.$$

In the further course, various Hamiltonians will play a role. For the purpose of distinction, from now on, the Hamiltonian operator from Equation (1) is denoted by the symbol  $\mathbf{H}^R$ . Here, 'R' stands for 'Rotor'. Since the two kets  $|0\rangle$  and  $|1\rangle$  are eigenstates of  $\mathbf{H}^R$  and orthonormal, the matrix  $\underline{H}^R$  can be explicitly specified:

$$\underline{H}^R = \begin{pmatrix} E_1 & 0 \\ 0 & E_2 \end{pmatrix}.$$

This simple result can also be presented more awkwardly, which will prove advantageous later:

$$\underline{H}^R = \frac{1}{2} \begin{pmatrix} E_1 + E_2 & 0 \\ 0 & E_1 + E_2 \end{pmatrix} + \frac{1}{2} \begin{pmatrix} E_1 - E_2 & 0 \\ 0 & -(E_1 - E_2) \end{pmatrix}.$$

Using the identity matrix  $\underline{1}$  and the Pauli matrix  $\underline{\sigma}_z$ , this formula can be compactly written as

$$\underline{H}^R = \frac{1}{2}(E_1 + E_2)\underline{1} + \frac{1}{2}(E_1 - E_2)\underline{\sigma}_z.$$

When this matrix is used to determine the time evolution of the qubit state using Equation (17), it turns out that the first term proportional to  $\underline{1}$  only contributes a phase factor to the solution  $\underline{\psi}(t)$ . Since such phase factors are meaningless in quantum physics, the first term can be simply omitted without relevant consequences. Thus, the matrix representing the Hamiltonian operator (1) can be written in the form

$$\underline{H}^R = -\frac{1}{2}\hbar\omega_1\underline{\sigma}_z. \tag{18}$$

Here, the energy difference  $E_1 - E_2 = -\Delta E_1$  has been expressed through  $\omega_1$  using Equations (10).

### 6.2. The Driven Rotor

The Hamiltonian for the interaction of a radiation field with the rotor is given by the dipole approximation:

$$H^W = -e\vec{r} \cdot \vec{E}$$

( $e$  elementary charge) (In terms of electrodynamics, the rotor-ion described at the beginning of Section 2 is composed of an electric monopole and an electric dipole. The dipole consists of a proton in the nucleus and the valence electron. The remaining protons form the monopole. Higher orders in the multipole expansion of the energy of the charge distribution in an external electric field are of minor importance (see [19] Section 4.2). The acceleration experienced by the comparatively massive monopole in the high-frequency laser field is neglected). For a transversely polarized radiation field propagating in the direction of the z-axis, this yields

$$H^W = -e(xE_x + yE_y) = -eR(E_x \cos \theta + E_y \sin \theta)$$

(see Figure 1). Specifically, for the field from Equation (9) (since  $L_z$  is not included in  $H^W(\theta)$ ), this becomes

$$H^W(\theta) = -eR\hat{E}(\cos(\theta) \cos(\omega t + \delta) + \sin(\theta) \sin(\omega t)). \tag{19}$$

The corresponding Hamiltonian operator is explicitly time-dependent:

$$\mathbf{H}^W(\boldsymbol{\theta}) = -eR\hat{E}(\cos(\boldsymbol{\theta}) \cos(\omega t + \delta) + \sin(\boldsymbol{\theta}) \sin(\omega t)),$$

which will be important for the calculation of the system's time evolution later. To form the matrix  $\underline{H} = \underline{H}^R + \underline{H}^W$  corresponding to the total Hamiltonian operator, the matrix representation of  $\mathbf{H}^W(\boldsymbol{\theta})$  in the  $|b\rangle$  basis must be computed. The four matrix elements  $\langle b|\mathbf{H}^W|b'\rangle$  can be determined using the completeness relation

$$\mathbf{1} = \int_0^{2\pi} |\theta\rangle\langle\theta|d\theta$$

and the property (This relationship can be easily proven using the power series expansion of the function  $f$ )

$$f(\mathbf{A})|a\rangle = f(a)|a\rangle$$

where  $f(\mathbf{A})$  is a function of the operator  $\mathbf{A}$  and  $|a\rangle$  is an eigenstate of  $\mathbf{A}$ . Thus,

$$\begin{aligned} \langle b|\mathbf{H}^W(\boldsymbol{\theta})|b'\rangle &= \int_0^{2\pi} \langle b|\mathbf{H}^W(\boldsymbol{\theta})|\theta\rangle\langle\theta|b'\rangle d\theta \\ &= \int_0^{2\pi} H^W(\theta)\langle b|\theta\rangle\langle\theta|b'\rangle d\theta \\ &= \int_0^{2\pi} H^W(\theta)\psi_b^*(\theta)\psi_{b'}(\theta) d\theta \end{aligned}$$

$(\langle b|\theta\rangle = \langle \theta|b\rangle^*)$ . Using Equations (7) and (19), the integrals can be computed easily. The resulting matrix is

$$\underline{H}^W = -\frac{1}{2}\hbar\Omega\cos(\omega t + \delta)\underline{\sigma}_x = -\frac{1}{2}\hbar\Omega\cos(\omega t + \delta)(\underline{\sigma}_+ + \underline{\sigma}_-) \tag{20}$$

with  $\Omega := e\hat{E}R/\hbar$ . Additionally, the matrices

$$\underline{\sigma}_- = \begin{pmatrix} 0 & 1 \\ 0 & 0 \end{pmatrix} \quad \text{and} \quad \underline{\sigma}_+ = \begin{pmatrix} 0 & 0 \\ 1 & 0 \end{pmatrix}$$

have been introduced. The decomposition of the Pauli matrix  $\underline{\sigma}_x$  into the two terms  $\underline{\sigma}_+$  and  $\underline{\sigma}_-$  may seem arbitrary here but is necessary for the following.

### 6.3. Product Ansatz

Now, the system of differential equations (17) needs to be solved (Since the system’s Hamiltonian is time-dependent, the procedure of superposing eigenstates as shown at the end of Section 2 doesn’t work ([16] Section 2.1)). An exact solution is not known, but there exists a good approximate solution based on a product ansatz of the form (The ansatz corresponds to the *Dirac* or *interaction picture* of quantum physics ([16] Section 5.5).)

$$\underline{\psi}(t) = \underline{R}_z^{-1}(\omega_1 t)\underline{\psi}^w(t). \tag{21}$$

As explained in Section 5,  $\underline{R}_z(\gamma)$ , applied to a column vector, causes a rotation of the column vector about the  $z$ -axis of the state space. In the present case, the rotation angle  $\gamma$  is proportional to time, and the angular velocity of the rotation is  $\omega_1$  (When considering the term neglected in Equation (18), the angular velocity is correspondingly larger.). According to Equation (16),  $\underline{R}_z^{-1}(\omega_1 t)$  causes a rotation with opposite direction of rotation compared to  $\underline{R}_z(\omega_1 t)$ .

Using the product ansatz in the differential equation system (17), the time derivative of  $\underline{\psi}(t)$  is required. With Equation (15) and the product rule, we get

$$\dot{\underline{\psi}}(t) = \dot{\underline{R}}_z^{-1}(\omega_1 t)\underline{\psi}^w(t) + \underline{R}_z^{-1}(\omega_1 t)\dot{\underline{\psi}}^w(t) = i\frac{\omega_1}{2}\underline{\sigma}_z\underline{R}_z^{-1}(\omega_1 t)\underline{\psi}^w(t) + \underline{R}_z^{-1}(\omega_1 t)\dot{\underline{\psi}}^w(t). \tag{22}$$

Substituting the right-hand sides of Equations (21) and (22) into the equation system (17) with  $\underline{H} = \underline{H}^R + \underline{H}^W$ , we obtain

$$-\frac{1}{2}\hbar\omega_1\underline{\sigma}_z\underline{R}_z^{-1}\underline{\psi}^w + i\hbar\underline{R}_z^{-1}\dot{\underline{\psi}}^w = (\underline{H}^R\underline{R}_z^{-1} + \underline{H}^W\underline{R}_z^{-1})\underline{\psi}^w. \tag{23}$$

Then, after multiplication by (see Equation (16))

$$\underline{R}_z(\omega_1 t) = \exp(-i\omega_1 t\underline{\sigma}_z/2)$$

from the left, we get

$$-\frac{1}{2}\hbar\omega_1\underline{R}_z\underline{\sigma}_z\underline{R}_z^{-1}\underline{\psi}^w + i\hbar\underline{\psi}^w = (\underline{R}_z\underline{H}^R\underline{R}_z^{-1} + \underline{R}_z\underline{H}^W\underline{R}_z^{-1})\underline{\psi}^w. \tag{24}$$

Since

$$\underline{R}_z\underline{H}^R\underline{R}_z^{-1} = -\frac{1}{2}\hbar\omega_1\underline{R}_z\underline{\sigma}_z\underline{R}_z^{-1}$$

(see Equation (18)), the first two terms on both sides of Equation (24) cancel out. By explicit calculation, we get

$$\underline{R}_z(\alpha)\underline{\sigma}_\pm\underline{R}_z^{-1}(\alpha) = \exp(\pm i2\alpha)\underline{\sigma}_\pm. \tag{25}$$

Using Equations (20) and (25), the differential equation system (24) becomes

$$i\hbar\underline{\psi}^w(t) = -\frac{1}{2}\hbar\Omega\cos(\omega t + \delta)[e^{+i\omega_1 t}\underline{\sigma}_+ + e^{-i\omega_1 t}\underline{\sigma}_-]\underline{\psi}^w(t). \tag{26}$$

Now, we use Euler’s formula to rephrase the cosine function and obtain

$$\cos(\omega t + \delta) = \frac{1}{2} [e^{+i(\omega t + \delta)} + e^{-i(\omega t + \delta)}] = \frac{1}{2} [e^{+i\delta} e^{+i\omega t} + e^{-i\delta} e^{-i\omega t}].$$

With this, the factor appearing on the right side of Equation (26) can be reformulated as

$$2\cos(\omega t + \delta)[e^{+i\omega_1 t} \underline{\sigma}_+ + e^{-i\omega_1 t} \underline{\sigma}_-] = e^{+i\delta} e^{+i(\omega + \omega_1)t} \underline{\sigma}_+ + e^{+i\delta} e^{+i(\omega - \omega_1)t} \underline{\sigma}_- + e^{-i\delta} e^{-i(\omega - \omega_1)t} \underline{\sigma}_+ + e^{-i\delta} e^{-i(\omega + \omega_1)t} \underline{\sigma}_-. \tag{27}$$

#### 6.4. Rotating Wave Approximation

Next, let's examine what happens when the laser frequency approaches the resonant frequency of the rotor transition  $\omega \rightarrow \omega_1$ . It's clear that in this case, the amplitudes of the resonant terms (terms containing  $\omega - \omega_1$ ) become large. The non-resonant terms (those containing  $\omega + \omega_1$ ) become less significant and can be neglected (Rotating Wave Approximation (RWA), see [18] Section 4.2 and [20] Section 5.1.2). In this approximation, we now consider the resonant case  $\omega = \omega_1$ . Equation (27) then approximately reduces to

$$2\cos(\omega_1 t + \delta)[e^{+i\omega_1 t} \underline{\sigma}_+ + e^{-i\omega_1 t} \underline{\sigma}_-] \approx e^{+i\delta} \underline{\sigma}_- + e^{-i\delta} \underline{\sigma}_+.$$

With the simplified differential equation system (26) under the RWA,

$$i\underline{\dot{\psi}}^w(t) = -\frac{1}{4}\Omega[e^{+i\delta} \underline{\sigma}_- + e^{-i\delta} \underline{\sigma}_+]\underline{\psi}^w(t)$$

is easy to solve. The solution can be expressed in the form

$$\underline{\psi}^w(t) = \underline{U}^w(t)\underline{\psi}^w(0) \tag{28}$$

with

$$\underline{U}^w(t) := \begin{pmatrix} \cos(\Omega t/4) & ie^{i\delta} \sin(\Omega t/4) \\ ie^{-i\delta} \sin(\Omega t/4) & \cos(\Omega t/4) \end{pmatrix}.$$

Our task is to determine  $\underline{\psi}(t)$ . This column vector can be obtained with Equation (21) and Equation (28) as

$$\underline{\psi}(t) = \underline{R}_z^{-1}(\omega_1 t)\underline{U}^w(t)\underline{\psi}^w(0).$$

Clearly  $\underline{\psi}^w(0) = \underline{\psi}(0)$ , and thus, we achieve our goal:

$$\underline{\psi}(t) = \underline{U}(t)\underline{\psi}(0)$$

with  $\underline{U}(t) := \underline{R}_z^{-1}(\omega_1 t)\underline{U}^w(t)$ . In matrix form, we have

$$\underline{U}(t) = \begin{pmatrix} e^{i\omega_1 t/2} \cos(\Omega t/4) & ie^{i(\omega_1 t/2 + \delta)} \sin(\Omega t/4) \\ ie^{-i(\omega_1 t/2 + \delta)} \sin(\Omega t/4) & e^{-i\omega_1 t/2} \cos(\Omega t/4) \end{pmatrix}. \tag{29}$$

As claimed in Section 5, the same matrix can be obtained by successively applying two rotation matrices. One of several possibilities for this is

$$\underline{U}(t) = \underline{R}_z(\gamma_3)\underline{R}_y(\gamma_2)\underline{R}_z(\gamma_1)$$

with

$$\gamma_1 = \delta + \pi/2, \quad \gamma_2 = -\Omega t/2, \quad \gamma_3 = -(\omega_1 t + \delta + \pi/2). \tag{30}$$

### 7. 1-Qubit Gates

The matrix  $\underline{U}(t)$  from Equation (29) allows us to calculate the effect of the radiation field from Equation (9) on the state of a qubit. The result evidently depends on the chosen parameters. The frequency  $\omega$  is fixed to  $\omega_1$  by the properties of the rotor. To achieve a specific effect of the field on the qubit (i.e., to realize a gate),  $\hat{E}$ ,  $\delta$ , and the duration of the irradiation  $t$  remain as parameters. This will now be demonstrated conclusively using two important gates.

### 7.1. Quantum-NOT Gate

Quantum gates are defined by their effect on the basis states  $|0\rangle$  and  $|1\rangle$  (see [6] Section 1.3). The first example where we want to test our hard-earned result from Equation (29) is the Quantum-NOT gate. The associated operator  $X$  is defined by

$$X|0\rangle = |1\rangle \text{ and } X|1\rangle = |0\rangle.$$

Therefore, applying  $X$  on the general state  $|\psi\rangle = \psi_0|0\rangle + \psi_1|1\rangle$  results in

$$|\phi\rangle = X|\psi\rangle = X(\psi_0|0\rangle + \psi_1|1\rangle) = \psi_0X|0\rangle + \psi_1X|1\rangle$$

i.e.,

$$|\phi\rangle = \psi_1|0\rangle + \psi_0|1\rangle$$

(swapping the coefficients).

The column vectors corresponding to  $|\psi\rangle$  and  $|\phi\rangle$  are

$$\underline{\psi} = \begin{pmatrix} \psi_0 \\ \psi_1 \end{pmatrix} \text{ and } \underline{\phi} = \begin{pmatrix} \psi_1 \\ \psi_0 \end{pmatrix}.$$

It is easy to see that the relation  $\underline{\phi} = \underline{X}\underline{\psi}$  is accomplished by the matrix

$$\underline{X} = \underline{\sigma}_x = \begin{pmatrix} 0 & 1 \\ 1 & 0 \end{pmatrix}.$$

To obtain the corresponding parameters of the laser radiation field, we can compare the matrix from Equation (29) with  $\underline{X}$ . We start in the upper left:

$$U_{00}(t) = e^{i\omega_1 t/2} \cos(\Omega t/4) = 0.$$

Since  $e^{i\omega_1 t/2} \neq 0$ , it follows that  $\cos(\Omega t/4) = 0$  must hold. The simplest solution to this equation is  $\Omega t/4 = \pi/2$ , i.e.,

$$t = t_x = \frac{2\pi\hbar}{e\hat{E}R}.$$

Since  $X_{01} = X_{10}$ , it follows that  $U_{01}$  has to be equal to  $U_{10}$ . After canceling the sine factor,

$$\pi \frac{\omega_1}{\Omega} + \delta = -\left(\pi \frac{\omega_1}{\Omega} + \delta\right).$$

This implies

$$\delta = \delta_x = -\pi \frac{\omega_1}{\Omega} = -\frac{3\pi\hbar^2}{2em\hat{E}R^3}.$$

Substituting the results for  $t$  and  $\delta$  into the matrix from Equation (29), we get

$$\underline{U}(t_x) = i \begin{pmatrix} 0 & 1 \\ 1 & 0 \end{pmatrix} = i\underline{X}.$$

Thus, if the rotor is irradiated with the laser for the duration  $t_x$ , the effect on the associated qubit is, up to a phase factor of  $i$ , that of a Quantum-NOT gate, when the phase shift  $\delta$  is set to  $\delta_x$ . Since phase factors have no physically detectable effects, we have successfully constructed the desired gate.

For the rotation angles according to Equations (30), we obtain

$$\gamma_1 = \delta_x + \frac{\pi}{2}, \quad \gamma_2 = -\pi, \quad \gamma_3 = \delta_x - \frac{\pi}{2}.$$

We consider two examples:

Example 1. Let the initial state be  $|\psi\rangle = |0\rangle$ . The associated Bloch vector is  $\vec{b} = (0,0,1)^T$ . After applying the gate, the resulting state is  $|1\rangle$  with the Bloch vector  $\vec{b}' = (0,0,-1)^T$ . The effect of the gate corresponds to rotations

1. around the  $z$ -axis (no effect for this initial state, so  $\vec{b} \rightarrow \vec{b}$ ),

2. around the  $y$ -axis (rotation angle  $\gamma_2 = -\pi$ , i.e.,  $\vec{b} \rightarrow \vec{b}'$ ),
3. around the  $z$ -axis (no effect for this intermediate state, i.e.,  $\vec{b}' \rightarrow \vec{b}'$ ).

Example 2. Now, let the initial state be  $|\psi\rangle = \frac{1}{\sqrt{2}}(|0\rangle + |1\rangle)$ . The associated Bloch vector is  $\vec{b} = (1,0,0)^T$ . As mentioned above, the gate swaps the coefficients. Since they are equal, the state does not change under the effect of the gate. For simplicity, let's assume that the radiation field can be approximately described by  $\delta_x = 0$  ( $\omega_1 \ll \Omega$ ).

The following rotations need to be performed:

1. Around the  $z$ -axis, rotation angle  $\gamma_2 = \pi/2$  (the Bloch vector becomes  $(0,1,0)^T$ ),
2. around the  $y$ -axis (no effect for this intermediate state),
3. around the  $z$ -axis, rotation angle  $\gamma_3 = -\pi/2$ : The Bloch vector returns to  $(1,0,0)^T$ .

In both examples, it is shown that the rotational angle formalism is consistent with our expectations.

### 7.2. Hadamard Gate

The procedure for the widely used Hadamard gate  $G$  is analogous (To avoid confusion with a Hamiltonian operator, we use the symbol  $G$ ). The definition of the gate using the two basis states is

$$G|0\rangle = \frac{1}{\sqrt{2}}(|0\rangle + |1\rangle) \quad \text{and} \quad G|1\rangle = \frac{1}{\sqrt{2}}(|0\rangle - |1\rangle).$$

For the general state  $|\psi\rangle$ , this results in

$$\begin{aligned} |\phi\rangle &= G|\psi\rangle = G(\psi_0|0\rangle + \psi_1|1\rangle) = \psi_0 G|0\rangle + \psi_1 G|1\rangle \\ &= \frac{\psi_0}{\sqrt{2}}(|0\rangle + |1\rangle) + \frac{\psi_1}{\sqrt{2}}(|0\rangle - |1\rangle) \end{aligned}$$

i.e.,

$$|\phi\rangle = \frac{\psi_0 + \psi_1}{\sqrt{2}}|0\rangle + \frac{\psi_0 - \psi_1}{\sqrt{2}}|1\rangle.$$

The column vectors corresponding to  $|\psi\rangle$  and  $|\phi\rangle$  are

$$\underline{\psi} = \begin{pmatrix} \psi_0 \\ \psi_1 \end{pmatrix} \quad \text{and} \quad \underline{\phi} = \frac{1}{\sqrt{2}} \begin{pmatrix} \psi_0 + \psi_1 \\ \psi_0 - \psi_1 \end{pmatrix}$$

and the matrix corresponding to  $G$  is

$$\underline{G} = \frac{1}{\sqrt{2}} \begin{pmatrix} 1 & 1 \\ 1 & -1 \end{pmatrix}.$$

This matrix is again to be compared with that from Equation (29). We start with the main diagonal. There,  $U_{11} = -U_{00}$  must hold, and consequently,

$$e^{i\frac{\omega_1 t}{2}} \cos\left(\frac{\Omega t}{4}\right) = -e^{-i\frac{\omega_1 t}{2}} \cos\left(\frac{\Omega t}{4}\right).$$

After canceling the cosine factor and using  $-1 = e^{i\pi}$ , we get  $\omega_1 t/2 = \pi - \omega_1 t/2$ . This yields the irradiation time

$$t = t_G = \frac{2\pi m R^2}{3\hbar}.$$

The reasoning for the counterdiagonal is similar. From  $G_{10} = G_{01}$  we conclude that  $U_{10}$  needs to be equal to  $U_{01}$ . Thus,

$$ie^{i(\omega_1 t_G/2 + \delta)} \sin(\Omega t_G/4) = ie^{-i(\omega_1 t_G/2 + \delta)} \sin(\Omega t_G/4).$$

After canceling common factors, the phase shift of the Hadamard gate can be specified:

$$\delta = \delta_G = -\frac{\pi}{2}$$

(linearly polarized wave, see Figure 3).

Another equation is  $U_{00} = U_{01}$ . Explicitly, this means

$$e^{i\omega_1 t_G/2} \cos(\Omega t_G/4) = e^{-i(\omega_1 t_G/2 + \delta_G)} \sin(\Omega t_G/4)$$

After canceling and using  $i = e^{i\pi/2}$ , we have

$$\cos\left(\frac{\Omega t_G}{4}\right) = \sin\left(\frac{\Omega t_G}{4}\right).$$

This equation is satisfied for  $\Omega t_G/4 = \pi/4$ . Substituting  $t_G$  yields  $\Omega = \omega_1$  or

$$\hat{E} = \hat{E}_G = \frac{3\hbar^2}{2emR^3}.$$

As a precaution, let us verify the result by substituting  $t_G, \delta_G$ , and  $\omega_1$  for  $\Omega$  into Equation (29). We obtain

$$\underline{U}(t_G) = \frac{i}{\sqrt{2}} \begin{pmatrix} 1 & 1 \\ 1 & -1 \end{pmatrix} = i\underline{G}.$$

This is the desired result except for the physically irrelevant phase factor  $i$ .

Finally, let's consider the formalism for the Hadamard gate according to Equations (30). For the rotation angles, the following values are obtained:

$$\gamma_1 = 0, \quad \gamma_2 = -\frac{\pi}{2}, \quad \gamma_3 = -\pi.$$

We limit ourselves to one example:

Example 3. Let the initial state be  $|\psi\rangle = |0\rangle$  with Bloch vector  $\vec{b} = (0,0,1)^T$ . After applying the Hadamard gate, it becomes the state  $\frac{1}{\sqrt{2}}(|0\rangle + |1\rangle)$  with Bloch vector  $\vec{b}' = (1,0,0)^T$ . The effect of the gate corresponds to rotations

1. around the  $z$ -axis (no effect due to rotation angle  $\gamma_1 = 0$ , i.e.,  $\vec{b} \rightarrow \vec{b}$ ),
2. around the  $y$ -axis (rotation angle  $\gamma_2 = -\pi/2$ , i.e.,  $\vec{b} \rightarrow -\vec{b}'$ ),
3. around the  $z$ -axis (rotation angle  $\gamma_3 = -\pi$ , i.e.,  $-\vec{b}' \rightarrow \vec{b}'$ ).

Again, the result corresponds to our expectations.

## 8. Conclusions

We have achieved an important milestone, namely the determination of a general formula for constructing arbitrary 1-qubit gates. To this end we have made a series of approximations: Firstly, we have utilized the model of a rigid rotor to describe an atom respectively an ion. Since we are interested in qualitative assertions and not in quantitative results this seems to be a valid procedure: The similarities of the energy spectrum of atoms and the rotor are certainly sufficient to justify this approximation. Secondly, we have treated the radiation field of the laser classically. This is justified by the success of the model only. Including a quantized electromagnetic field would complicate matters even further. Finally, we have made use of the RWA. The justification of this approximation has been given in the corresponding section. All in all it seems that these approximations are appropriate to address the matter discussed here.

In the second part of this article, we will focus on the construction of the CNOT gate. The CNOT gate is a 2-qubit gate of outstanding importance. This is because any quantum gate can be constructed by combining CNOT and 1-qubit gates (universality). At the end of Part 2 of this article, all the elements for building an ion trap quantum computer will be available.

Recently several research groups have reported results, which promise real progress concerning the scalability of ion trap quantum computers [21,22]. So it seems that ion trap-based quantum

computers are a good candidate for demonstrating quantum supremacy on practical relevant problems.

**Funding:** This research received no external funding.

**Acknowledgments:** I would like to express my heartfelt thanks to Prof. Dr. Gernot Münster for error corrections and suggestions for improvement. Furthermore, I would like to thank Prof. Dr. Bernard Zygelman for his positive feedback.

**Conflicts of Interest:** The authors declare no conflict of interest.

## References

1. Milburn, G.J.; Davies, P. *Schrödinger's machines: the quantum technology reshaping everyday life*. W. H. Freeman and company: New York, NY, USA, 1997.
2. Dowling, J.P.; Milburn, G.J. Quantum technology: The second quantum revolution. *Philos. Trans. R. Soc. A Math. Phys. Eng. Sci.* **2003**, *361*, 1655–1674.
3. Rieffel, E.G. Polak, W.H. *Quantum computing: A gentle introduction (scientific and engineering computation)*. The MIT Press: Cambridge, MA, USA, 2011, p.372.
4. Aaronson, S. Introduction to Quantum Information Science Lecture Notes, 2018. Available online: <https://www.scottaaronson.com/qclec.pdf> (accessed on 1 October 2025).
5. Zygelman, B. *A first introduction to quantum computing and information*. Springer International Publishing: Cham, Switzerland, 2025. <https://doi.org/10.1007/978-3-031-66425-0>.
6. Nielsen, M.A.; Chuang, I.L. *Quantum computation and quantum information*. Cambridge university press: Cambridge, England, 2010.
7. Quantum Computing Business. The Quantum Insider Projects \$1 Trillion in Economic Impact From Quantum Computing by 2035. Available online: <https://thequantuminsider.com/2024/09/13/the-quantum-insider-projects-1-trillion-in-economic-impact-from-quantum-computing-by-2035/> (accessed on 4 July 2025).
8. Shor, P.W. Algorithms for Quantum Computation: Discrete Logarithm and Factoring. Proceedings of 35th Annual Symposium on Foundations of Computer Science, Santa Fe, NM, USA, 20–22 November 1994, pp.124–134. <http://dx.doi.org/10.1109/sfcs.1994.365700>.
9. Gimeno, I.; Luis, F.; Marcuello, C.; Pallarés, M. C.; Lostao, A.; de Ory, M. C.; Gomez, A.; Granados, D.; Tejedor, I.; Natividad, E.; Urtizberea, A.; Roubeau, O. Localized Nanoscale Formation of Vanadyl Porphyrin 2D MOF Nanosheets and Their Optimal Coupling to Lumped Element Superconducting Resonators. *J. Phys. Chem. C* **2025**, *129*, 973–982. <https://doi.org/10.1021/acs.jpcc.4c07265>.
10. Pozo, I.; Huang, Z.; Lombardi, F.; Alexandropoulos, D. I.; Kong, F.; Slota, M.; Tkach, I.; Bennati, M.; Deng, J.-R.; Stawski, W.; Horton, P. N.; Coles, S. J.; Myers, W. K.; Bogani, L.; Anderson, H. L. *Chem* **2024**, *10*, 299–316. <https://doi.org/10.1016/j.chempr.2023.09.013>.
11. Kajita, M. *Ion Traps: A gentle introduction*. IOP Publishing: Bristol, UK, 2022.
12. Cirac, J.I.; Zoller, P. Quantum computations with cold trapped ions. *Phys. Rev. Lett.* **1995**, *74*, 4091–4094. <https://doi.org/10.1103/PhysRevLett.74.4091>.
13. Bruzewicz, C.D.; Chiaverini, J.; McConnell, R.; Sage, J.M. Trapped-Ion Quantum Computing: Progress and Challenges. *Appl. Phys. Rev.* **2019**, *6*, 021314, <https://doi.org/10.1063/1.5088164>.
14. Bernardini, F.; Chakraborty, A.; Ordóñez, C.R. Quantum computing with trapped ions: a beginner's guide. *Eur. J. Phys.* **2023**, *45*, 013001, <https://doi.org/10.1088/1361-6404/ad06be>.
15. Susskind, L.; Hrabovsky, G. *Classical Mechanics: The Theoretical Minimum*. Penguin Books: London, UK, 2013.
16. Sakurai, J.J.; Napolitano, J. *Modern quantum mechanics*, 2nd ed.; Cambridge University Press: Cambridge, United Kingdom, 2020.
17. Kreyszig, E. *Advanced engineering mathematics*, 7th ed.; John Wiley & Sons, Inc.: New York, NY, USA, 1993.
18. Gerry, C.C.; Knight, P. *Introductory quantum optics*. Cambridge University Press: Cambridge, England, 2008.
19. Jackson, J.D. *Classical electrodynamics*, 3rd ed.; Wiley: Singapore, Singapore, 2021.
20. Steck, D.A. Quantum and Atom Optics. Revision 0.13.4. Available online: <Http://steck.us/teaching> (accessed on 8 July 2024).

21. Guo, W.X.; Zhang, C.; Qi, B.X.; Zhou, Z.C.; He, L.; Duan, L.M. A site-resolved two-dimensional quantum simulator with hundreds of trapped ions. *Nature* **2024**, *630*, 613–618, <https://doi.org/10.1038/s41586-024-07459-0>.
22. Jain, S.; Sägesser, T.; Hrmo, P.; Torkzaban, C.; Stadler, M.; Oswald, R.; Axline, C.; Bautista-Salvador, A.; Ospelkaus, C.; Kienzler, D.; et al. Penning micro-trap for quantum computing. *Nature* **2024**, *627*, 510–514, <https://doi.org/10.1038/s41586-024-07111-x>.



© 2025 by the authors. This article is an open access article distributed under the terms and conditions of the Creative Commons Attribution (CC BY) license (<http://creativecommons.org/licenses/by/4.0/>).